# Condensed Graphitic Carbon Nitride Nanorods by Nanoconfinement: Promotion of Crystallinity on Photocatalytic Conversion

Xin-Hao Li,*[†] Jinshui Zhang,[†,‡] Xiufang Chen,[†,‡] Anna Fischer,[§] Arne Thomas,[§] Markus Antonietti,[†] and Xinchen Wang[†,‡]

[†]Department of Colloid Chemistry, Max-Planck Institute of Colloids and Interfaces, Research Campus Golm, Potsdam 14476, Germany
[‡]Research Institute of Photocatalysis, State Key Laboratory Breeding Base of Photocatalysis, Fuzhou University, Fuzhou 350002, P. R. China
[§]Department of Chemistry, Technische Universität Berlin, Englische Strasse 20, Berlin 10587, Germany

Ⓢ Supporting Information

**ABSTRACT:** Photoactive, condensed carbon nitride nanorods (CNRs) can be obtained via confined thermal condensation of cyanamide inside the nanochannels of an anodic alumni oxide (AAO) membrane template. The promotion of a more condensed network of CNRs with lowered HOMO in water splitting (including both $H_2$ and $O_2$ revolution) and photocurrent output was demonstrated.

**KEYWORDS:** template synthesis, layered materials, carbon nitrides, crystal structure, photocatalysis
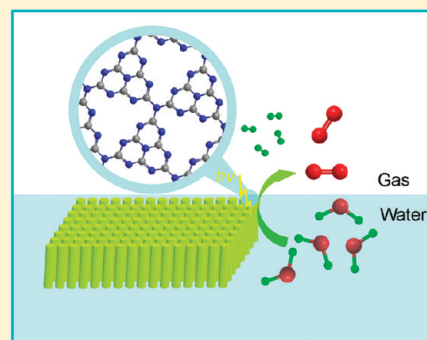
## INTRODUCTION

The development of semiconductor photocatalysts that can harvest visible light, transfer it into reactive charge couples, split the water molecules into hydrogen and oxygen, and simultaneously stay stable in water remains a key target of modern material science, reactualized as a result of renewable energy and environmental issues.[1−6] During the past three decades, a range of materials have been explored as semiconductor photocatalysts, which, thus far, still suffer from the general limitations of low quantum yield and low utilization efficiency of sunlight.[1] Meanwhile, research efforts include side conditions such as sustainability and scalability, and they redirected the search to earth-abundance photosensitizers as solar energy transducers and to coupling those with fuel-generation cascade reactions, such as water splitting[1] and $CO_2$ fixation,[2] to make energy-rich chemicals.

Binary carbon nitrides are sustainable materials containing carbon and nitrogen, only. They have long-been predicted to exhibit remarkable mechanical and electronic properties, and multiple functions as well.[3] Among various covalent CN allotropes, graphic carbon nitride (g-$C_3N_4$) is the most stable phase under ambient conditions, and it was introduced as a metal-free heterogeneous catalyst for both green synthetic chemistry and solar energy conversion.[4] As a "sustainable" material, carbon nitrides can be made via the thermal polycondensation of simple N-containing monomers such as urea and cyanamide (again, made of ammonia and $CO_2$, only) at the price of a typical mass polymer. Considering the high thermal and chemical stabilities of g-$C_3N_4$ against oxidation together with its semiconductor properties and low cost of mass production, g-$C_3N_4$ based materials are potentially close to an

ideal candidate for a solar energy conversion system.[5] To this end, we have analyzed the general implication of g-$C_3N_4$ in a heterogeneous photocatalysis, and we have found that even the first generation g-$C_3N_4$ systems can catalyze water reduction/ oxidation, organic photosynthesis, and degradation of dye molecules with visible light, but still with moderate performance, only.

Being considered as an organic semiconductor in nature, there are plentiful choices of modification schemes for g-$C_3N_4$ including both inorganic and organic protocols. The structure and composition of g-$C_3N_4$ have been finely engineered for enhancing photocatalytic/catalytic performance by either doping (e.g., B, C, F, Fe, and P) or copolymerization that allows for the tuning of polymeric subunits at the molecular level.[6] The HOMO/ LUMO positions, the band gap, and, hence, the photocatalytic performance of carbon nitride polymer are therefore more adjustable than that of classical inorganic semiconductors. Additional textural modification of the functional g-$C_3N_4$ materials is still envisaged by templating with nanostructured silica, followed by the removal of silica with HF. All these modifications lead to an enhancement in photocatalytic activity for $H_2$ evolution over the unmodified material; however, no significant enhancement in $O_2$ evolution has been reported, presumably as a result of the moderate water oxidation ability of g-$C_3N_4$ based photocatalysts. We and others reported a sulfur-mediated approach to synthesize carbon nitride polymers that were found to promote the $O_2$ revolution

rate as a result of their lower intrinsic valence band (HOMO) positions (200 mV lower than normal g-$C_3N_4$) due to more condensed carbon nitride graphene sheets.[6d,e]

An alternative approach to achieve improved photoelectric performance is improving the crystallinity of g-$C_3N_4$, which can, in principle, promote the kinetics of charge diffusion in both the bulk and the surface. Conventional photoactive g-$C_3N_4$ is a polymeric, slightly distorted solid prepared via bulk polycondensation at high temperature, which usually leads to incomplete polymerization or condensation with $-NH_2$ groups left. These $-NH_2$ motifs as defects in the plane of graphitic carbon nitride could principally lead to sub-band gap absorption and, thus, a narrower band gap with HOMO levels increased. Highly condensed g-$C_3N_4$ is thought to have higher carrier mobility and lower HOMO levels, presumably as a result of fewer defects in the network, promising access to improved oxidation power. High-crystalline graphitic carbon nitride can be obtained via a thermal condensation reaction in a melt salt medium to overcome the kinetics limitations of bulk polymerization, but the resulting g-$C_3N_4$ was virtually inactive, likely as a result of the secondary change of semiconductor structure.[4e] Translating the bulk polycondensation into nanodimensional volume is considered an alternative to address the kinetics problems by enhancing the mobility of the confined polymer, which, in addition, offers a direct tool toward the nanofabrication of carbon nitride heterostructures with improved charge separation and collection.

Principally, the nanoscale processing of polymers and glasses in confining geometries with dimensions approaching the radius of gyration or the cooperative length of the system can strikingly influence the polymer's mobility, phase behaviors, orientation, and chain conformation, as a result of confinement-induced entropy loss, interfacial interactions, structural symmetry breaking, and surface bonding.[7] Porous anodic alumina oxide (AAO) membranes have been widely applied to study the confinement effect on the crystallization and morphology evolution of polymers, polymer-templated materials, and inorganic materials in confined dimensions.[7–9] For example, a bulk-phase lamella-forming block-copolymer in cylindrical channels of a porous AAO template was demonstrated to form concentric cylinder nanorods with a rich variety of novel oriented morphologies.[7] As a second example, the confined assembly of silica—copolymer composites resulted in oriented mesostructures with chiral mesopores such as single- and double-helical geometries spontaneously formed inside the alumina nanochannels.[8] Moreover, highly ordered $TiO_2$ single-crystalline nanowires arrays can also be fabricated within the pores of the AAO template.[9a]

It is, therefore, scientifically promising to perform the bulk condensation of g-$C_3N_4$ into empty alumina membranes, not only to fabricate highly condensed and oriented g-$C_3N_4$ but also to obtain light-harvesting semiconductor nanorod arrays with directional charge transport properties as building blocks for artificial photosynthesis devices, as exemplified with the well-described cases of $TiO_2$- and Si-based nanorod arrays.[10] Such architectures are known to separate photon absorption and charge-carrier collection into orthogonal spatial directions. Further fabrication of radial heterojunctions in these semiconductor nanorods can, in principle, enable optical absorption along the longer axial dimension to maximize light-harvesting, while charge carrier extraction would take place over the much shorter radial dimension (typically smaller than the minority-carrier diffusion length) to promote charge separation (Scheme 1 bottom right). By optimizing the wire length and the diameter of the nanostructures,

**Scheme 1. AAO Templating Approaches toward CNRs via Three Steps: (1) Filling the AAO Template (Gray) with Monomer Cyanamide (White); (2) Heating the Filled Templates at 600 °C under $N_2$ Flow for 4 h; and (3) Etching the Template to Release CNRs (Yellow)** [a]
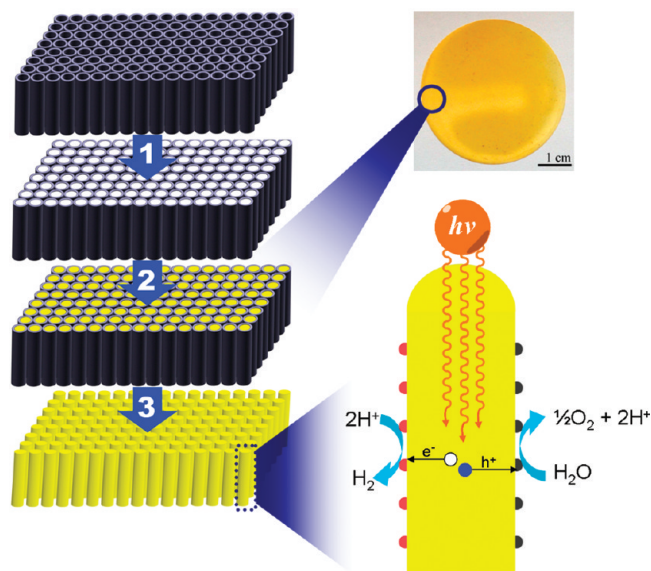


[a] Top right: photograph of CNRs in AAO before removing the template. Bottom right: proposed reaction mechanism of water oxidation and reduction.

the facile control of the optical absorption and charge kinetics could, in principle, be optimized to adopt the geometry needed for the tasks of the respective solar devices.

In this paper, we, therefore, use AAO templates to physically confine the synthesis of g-$C_3N_4$ rods (CNRs) by a thermal condensation of cyanamide inside individual nanochannels. We demonstrated the confinement effect of the AAO template on enhancing both the orientation and the crystallinity of g-$C_3N_4$. The highly condensed and oriented CNRs show a more ideal C/N molecular ratio, presumably due to fewer $NH_2$-groups and a lower HOMO level. As expected, CNRs are photoactive and exhibit enhanced photocatalytic performance, especially the water oxidation ability, over less-condensed g-$C_3N_4$.

## ■ EXPERIMENTAL SECTION

**Synthesis of CNRs.** The AAO templates (Whatman Anodisc 47, 0.2 $\mu$m) are immersed in a homogeneous mixture of 10 g of cyanamide and 5 g of distilled water and degassed under sonication with a power of 100 W for 10 min. The filled AAO templates, the outer surfaces of which were thoroughly cleaned with filter papers, were heated at a temperature of 600 °C for 4 h (ramp: 2.5 °C min$^{-1}$) under the protection of $N_2$. The CNRs were released by chemically etching the AAO with 1 M HCl solution for 72 h, washing with more HCl solution and distilled water, and separation via centrifugation.

**Characterization.** XRD measurements were performed on a Bruker D8 diffractometer operating with Cu K$\alpha_1$ radiation. UV—vis spectra were recorded using a Varian Cary 500 Scan UV—vis system equipped with a Labsphere diffuse reflectance accessory. Fourier transform infrared (FTIR) spectra were recorded on a BioRad FTS 6000 spectrometer. Transmission electron microscopy (TEM) was recorded on a Zeiss 920
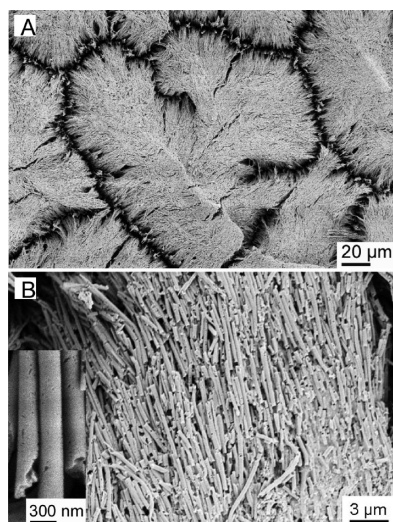
**Figure 1.** SEM images of CNRs.

microscope, and scanning electron microscopy (SEM) was performed on a LEO 1550-Gemini instrument.

**Experimental Details.** Photocatalytic reactions were carried out in a Pyrex top-irradiation reaction vessel connected to a glass closed gas circulation system. $H_2$ revolution analysis was performed by dispersing 50 mg of catalyst powder in an aqueous solution (100 mL) containing triethanolamine (10 mL) as the sacrificial electron donor and 3 wt % Pt as the cocatalyst. For the $O_2$ production reaction, 50 mg of catalyst powder was dispersed in an aqueous solution (100 mL) containing $AgNO_3$ (0.01 M as an electron acceptor and $La_2O_3$ (0.2 g) as a pH buffer agent. The reactant solution was evacuated several times to remove air completely before the photocatalytic reaction. A 300 W xenon lamp was applied as the light source, and visible light irradiation was realized by using a 420 nm cutoff filter. The temperature of the reactant solution was maintained at room temperature by a flow of cooling water during the reaction. The evolved gases were analyzed by gas chromatography.

## ■ RESULTS AND DISCUSSION

As shown in Scheme 1, a three-step method was applied to prepare the CNRs with the assistance of a hard template AAO. As a result of their high porosity and the high stability against heat treatment at relatively high temperatures, AAO templates are ideal for thermally condensing monomers to g-$C_3N_4$. In the photograph (Scheme 1 top right) of CNRs in AAO, the homogeneous distribution of the CNRs in the AAO templates is evidenced. After removing AAO templates by acid etching (1 M HCl), CNRs with a mean diameter of 260 nm were obtained, as shown in Figure 1. No bulk-phase g-$C_3N_4$ was observed before and after the removal of AAO templates (Figure S1). The diameter of the CNR is in good agreement with the pore size of the AAO. Unlike the bulk phase of g-$C_3N_4$, with a slightly distorted lamellar structure, the polymeric network of CNRs seems to be highly condensed, as only nanorods with smooth surfaces can be seen in the corresponding SEM image (Figure 1B). It is interesting to note that the CNR form, while drying, spontaneously highly organized superstructures (Figure 1A), which clearly evidence anisotropic mutual interactions and the ability to self-assemble. The X-ray diffraction (XRD) pattern of the CNRs (Figure 2) further reveals the improvement of the condensation structure. The strong characteristic interplanar stacking peak of aromatic systems of CNRs, indexed for graphitic materials as
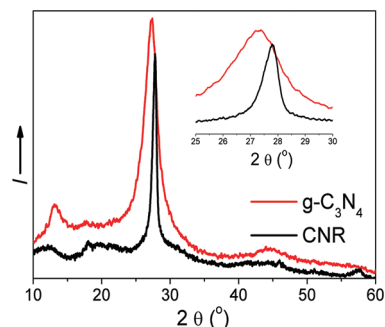


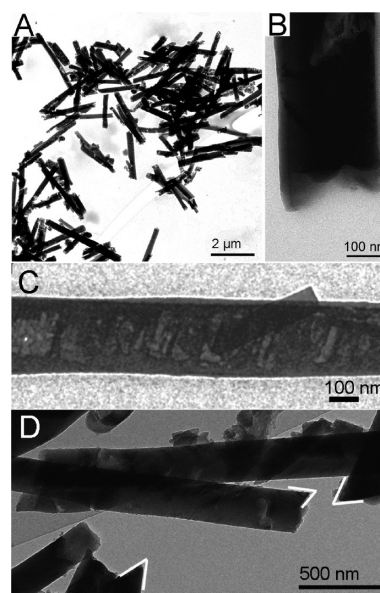**Figure 2.** XRD patterns of CNRs and bulk g-$C_3N_4$.



**Figure 3.** TEM images of CNRs.

the (002) peak, slightly shifts from 27.3° (bulk phase) to 27.9°; that is, the average interlayer distance of the CNRs is significantly compressed to a smaller $d$ value ($d$ = 0.32 nm). The (002) peak of the CNRs simultaneously became much narrower with a full width at half-maximum (fwhm) of only 0.61°, revealing the increased degree of condensation and enhanced domain size.

It has been reported that the order of a polymeric network of undoped g-$C_3N_4$ can only be improved by isothermally tempering the precursor in a sealed quartz ampule at 600 °C for 10 h, while heat treatment in an open crucible with longer time or higher temperature only results in the residue-free disappearance of the material via the generation of nitrogen and dicyan fragments.[4d] Similar to the sealed quartz ampule, the channels of AAO are thought to act as microreactors, sealed by capillarity. The end of the channel can also be sealed by the as-formed g-$C_3N_4$ to keep the monomers and intermediate compounds from evaporation and decomposition.

The confinement effect of the alumina channels on the mesostructure of the polymeric network becomes more obvious in the transmission electron microscopy (TEM) observations. Carbon nitride obviously polymerizes first into a close-packed layer on the pore wall, thus resulting in a hollow tube structure (Figure 3B). Secondary polymerization along the as-formed layers as a nucleation center results in condensed secondary crystals with a ca. 76°
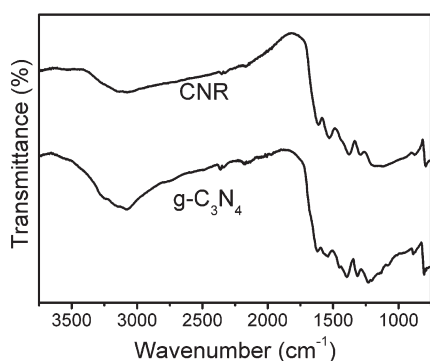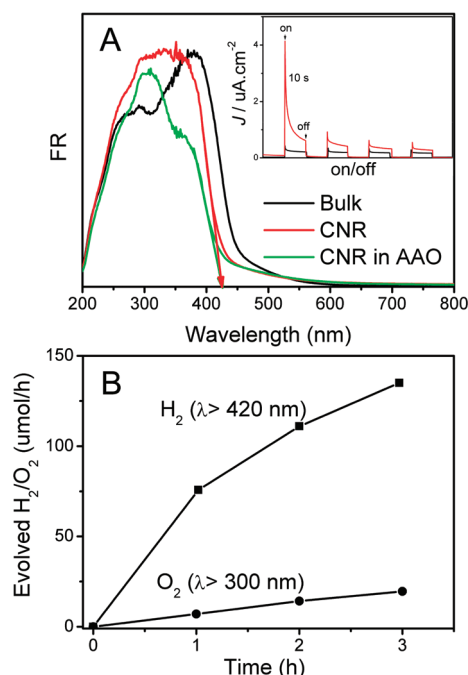
**Figure 4.** FTIR spectra of CNRs and bulk g-C$_3$N$_4$.



**Figure 5.** (A) Optical absorption spectra of CNRs and bulk g-C$_3$N$_4$; (inset) corresponding photocurrent out with a bias voltage of 0.2 V; and (B) hydrogen and oxygen revolution from water by CNRs.

orientation to the wall (Figure 3C). The sharp ends (Figures 3D and 1B) of broken CNRs further reveal their oriented and crystalline structure. According to the elemental analysis, the C/N molar ratio of CNRs is 0.72, significantly higher than that of bulk g-C$_3$N$_4$ (0.68) but still lower than the theoretical value (0.75) of a completely condensed species. The broad IR band around 3100 cm$^{-1}$, which is attributed to the presence of secondary and primary amines, became weak and less developed in the FTIR spectrum (Figure 4) of CNRs, as compared with that of bulk g-C$_3$N$_4$, while the characteristic aromatic CN heterocycles band (1200−1600 cm$^{-1}$) and the band breathing mode of the triazine units at 800 cm$^{-1}$ remained practically the same. All these observations speak for the formation of a more condensed polymeric network of CNRs with fewer −NH$_2$ and −NH− motifs.

The highly condensed structure results in high stability against acid or base etching. Protonated g-C$_3$N$_4$ solids with a broad XRD peak and blue-shift band gap are easily prepared by immersing bulk g-C$_3$N$_4$ in HCl solution (>1 M).[11] However, the as-prepared

CNRs withstand critical post-treatment (e.g., protonation by acid and corrosion by base) without decomposition or corrosion. Before and after removing the AAO templates, the CNRs exhibit the same optical band gap and, thereby, the same semiconductor properties, as shown in UV−vis spectra (Figure 3A). There is also no obvious change in both the width and the position of the (002) peak (Figure S2A in the Supporting Information) after immersing the CNRs in 85 wt % H$_3$PO$_4$, and 3 M NaOH, respectively, for 24 h, or in 1 M HCl for one week. As a control experiment, the width of the (002) peak of bulk g-C$_3$N$_4$ treated with 1 M NaOH for 24 h became broader (Figure S2B2 in the Supporting Information). All these observations illustrate the improved stability of the CNRs as a result of their higher degree of condensation and crystallinity.

As estimated from the UV/vis spectrum (Figure 5A), the optical band gap of CNRs shifts blue; that is, CNRs have a wider band gap. Considering that CNRs have the same composition as bulk g-C$_3$N$_4$ obtained under the same conditions and no heteroatoms are involved, it is reasonable to claim that CNRs exhibit a similar semiconductor structure as bulk g-C$_3$N$_4$ but exhibit an even lower HOMO position. This can be due to limiting the sub-band gap absorption, but it also can be due to an H-aggregate type intermolecular packing between the layers, resulting in a hypsochromic shift.[12]

CNR samples are photoactive, as confirmed by the photo-current measurement (Figure 5A inset). In addition, the in-plane carrier mobility is also improved in condensed and oriented CNRs, with fewer defects in the individual graphitic carbon nitride plane. As expected, the photocurrent output was increased by a factor of 2−9 for CNRs, although CNRs can absorb less visible light than bulk solids. After excluding the effect of the surface area of CNRs (25 m$^2$/g), the maximum value of the normalized photocurrent output is sill much higher than that of the bulk phase (10 m$^2$/g). These results clearly support the promotion of highly condensed structure in charge-carrier separation and in-plane mobility.

We further tested the photocatalytic performance of CNR samples in water splitting. CNRs indeed show an improvement in H$_2$ evolution activity under the irradiation of visible light ($\lambda$ > 420 nm). With 3 wt % Pt as the cocatalyst and triethanolamine as the sacrificial reagent, the H$_2$ evolution activity of CNRs (Figure 5B) is improved by a factor of ∼3 over that of the bulk g-C$_3$N$_4$ (28 $\mu$mol/h). Parts of the enhanced hydrogen activity could be ascribed to the enlarged surface area of the CNRs, as compared to that of bulk g-C$_3$N$_4$, not considering the decreased absorption of CNRs in visible light. As the reductive power is related to the LUMO position, this speaks for a practically slightly changed LUMO structure.

The promotion effect of the condensed structure therefore is much better seen by the lowered HOMO position and the coupled oxidation strength on the corresponding hole, here analyzed by the dioxygen producing half reaction. While mesoporous g-C$_3$N$_4$ (surface area 190 m$^2$/g, O$_2$ evolution rate 3.8 $\mu$mol/h) and the bulk phase (3.9 $\mu$mol/h) showed comparable activity not related to the surface area, O$_2$ evolution with CNRs was increased to a rate of 7 $\mu$mol/h, with all other parameters unaltered. Further electrochemical analysis (Figure S3 in the Supporting Information) of g-C$_3$N$_4$ and CNR samples revealed their band gap structure. As calculated from the $(ah\nu)^2$ versus photon energy plots,[6a] the estimated HOMO position of CNRs (roughly 1.76 V) is much lower than that of bulk phase (1.3 V), which is very close to the trend revealed by the photocatalytic performance.

## ■ CONCLUSIONS

To conclude, it was shown that the confined thermal condensation of cyanamide inside the channels of AAO templates is an efficient approach for increasing the crystallinity, extending domain size, and lowering the HOMO position of g-C$_3$N$_4$ based materials. The as-obtained CNRs offer a higher oxidation power, as exemplified by the O$_2$ revolution from water. The photocurrent output and H$_2$ revolution rate of CNRs were also enhanced, which we attribute to the improvement of condensation and orientation within the high aspect ratio nanowire structures. Further optimization of both optical absorption and charge-carriers separation can be envisaged by adjusting material nanostructures using an AAO membrane with different dimensions and pore sizes and/or different monomers to start the condensation. From the viewpoint of solar light usage, the hypsochromic shift following improved condensation was, of course, unwanted, but the implementation of J-type aggregation/order schemes is, in principle, in the hand of chemists[12] and will follow chemical variations.

Considering the facile modification of g-C$_3$N$_4$ by engineering the composition and surface functional groups, our synthetic method also promises a general approach for preparing other functional carbon nitride submicrometer rods with improved or new properties and extended applications, being a first step toward practical device fabrication based on carbon nitride photocatalysis.

## ■ ASSOCIATED CONTENT

**ⓢ Supporting Information.** SEM images and XRD patterns. This material is available free of charge via the Internet at http://pubs.acs.org.

## ■ AUTHOR INFORMATION

**Corresponding Author**
*E-mail: xin-hao.li@mpikg.mpg.de. Telephone: +49 (0)331 5679786.

## ■ ACKNOWLEDGMENT

## ■ REFERENCES

(1) For example, see: (a) Fujiashima, A.; Honda, K. *Nature* **1972**, *238*, 37. (b) Zou, Z. G.; Ye, J. H.; Sayama, K.; Arakawa, H. *Nature* **2001**, *414*, 625. (c) Maeda, K.; Teramura, K.; Lu, D.; Takata, T.; Saito, N.; Inoue, Y.; Domen, K. *Nature* **2006**, *440*, 295. (d) Ritterskamp, P.; Kuklya, A.; Wustkamp, M. A.; Kerpen, K.; Weidenthaler, C.; Demuth, M. *Angew. Chem., Int. Ed.* **2007**, *46*, 7770. (e) Osterloh, F. E. *Chem. Mater.* **2008**, *20*, 35. (f) Kudo, A.; Miseki, Y. *Chem. Soc. Rev.* **2009**, *38*, 253. (g) Yi, Z.; Ye, J.; Kikugawa, N.; Kako, T.; Ouyang, S.; Stuart-Williams, H.; Yang, H.; Cao, J.; Luo, W.; Li, Z.; Liu, Y.; Withers, R. *Nat. Mater.* **2010**, *9*, 559. (h) Liu, G.; Wang, L. Z.; Yang, H. G.; Cheng, H. M.; Lu, G. Q. *J. Mater. Chem.* **2010**, *20*, 831. (i) Chen, X.; Shen, S.; Guo, L.; Mao, S. S. *Chem. Rev.* **2010**, *110*, 6503.

(2) For example, see: (a) Shaikh, A.-A. G.; Sivaram, S. *Chem. Rev.* **1996**, *96*, 951. (b) Dalton, D. M.; Rovis, T. *Nat. Chem.* **2010**, *2*, 710. (d) Sakakura, T.; Choi, J.-C.; Yasuda, H. *Chem. Rev.* **2007**, *107*, 2365and references therein.

(3) (a) Liebig, J. *Ann. Pharm.* **1834**, *10*, 10. (b) Liu, A. Y.; Cohen, M. L. *Science* **1989**, *245*, 841. (c) Niu, C. M.; Lu, Y. Z.; Lieber, C. M. *Science* **1993**, *261*, 334.

(4) (a) Zhang, Z.; Leinenweber, K.; Bauer, M.; Garvie, L. A. J.; Mc-Millan, P. F.; Wolf, G. H. *J. Am. Chem. Soc.* **2001**, *123*, 7788. (b) Kroke, E.; Schwarz, M. *Coord. Chem. Rev.* **2004**, *248*, 493. (c) Vinu, A.; Ariga, K.; Mori, T.; Nakanishi, T.; Hishita, S.; Golberg, D.; Bando, Y. *Adv. Mater.* **2005**, *17*, 1648. (d) Thomas, A.; Fischer, A.; Goettmann, F.; Antonietti, M.; Müller, J.-O.; Schlögl, R.; Carlsson, J. M. *J. Mater. Chem.* **2008**, *18*, 4893. (e) Bojdys, M. J.; Müller, J.-O.; Antonietti, M.; Thomas, A. *Chem.—Eur. J.* **2008**, *14*, 8177. (f) Lee, J. S.; Wang, X. Q.; Luo, H. M.; Dai, S. *Adv. Mater.* **2010**, *22*, 1004. (g) Zou, X. X.; Li, G. D.; Wang, Y. N.; Zhao, J.; Yan, C.; Guo, M. Y.; Li, L.; Chen, J. S. *Chem. Commun.* **2011**, *47*, 1066.

(5) (a) Goettmann, F.; Thomas, A.; Antonietti, M. *Angew. Chem., Int. Ed.* **2007**, *46*, 2717. (b) Wang, X. C.; Maeda, K.; Thomas, A.; Takanabe, K.; Xin, G.; Carlsson, J. M.; Domen, K.; Antonietti, M. *Nat. Mater.* **2009**, *8*, 76. (c) Su, F. Z.; Mathew, S. C.; Lipner, G.; Fu, X. Z.; Antonietti, M.; Blechert, S.; Wang, X. C. *J. Am. Chem. Soc.* **2010**, *132*, 16299.

(6) (a) Zhang, J. S.; Chen, X. F.; Takanabe, K.; Maeda, K.; Domen, K.; Epping, J. D.; Fu, X. Z.; Antonietti, M.; Wang, X. C. *Angew. Chem., Int. Ed.* **2010**, *49*, 441. (b) Zhang, Y. J.; Mori, T.; Ye, J. H.; Antonietti, M. *J. Am. Chem. Soc.* **2010**, *132*, 6294. (c) Wang, Y.; Zhang, J. S.; Wang, X. C.; Antonietti, M.; Li, H. R. *Angew. Chem., Int. Ed.* **2010**, *49*, 3356. (d) Liu, G.; Niu, P.; Sun, C. H.; Smith, S. C.; Chen, Z. G.; Lu, G. Q.; Cheng, H.-M. *J. Am. Chem. Soc.* **2010**, *132*, 11642. (e) Zhang, J. S.; Sun, J. H.; Maeda, K.; Domen, K.; Liu, P.; Antonietti, M.; Fu, X. Z.; Wang, X. C. *Energy Environ. Sci.* **2011**, *4*, 675. (f) Li, X. H.; Chen, J. S.; Wang, X. C.; Sun, J. H.; Antonietti, M. *J. Am. Chem. Soc.* **2011**, *133*, 8074.

(7) Shin, K.; Xiang, H. Q.; Moon, S. I.; Kim, T.; McCarthy, T. J.; Russell, T. P. *Science* **2004**, *306*, 76.

(8) (a) Wu, Y.; Cheng, G.; Katsov, K.; Sides, S. W.; Wang, J.; Tang, J.; Fredrickson, G. H.; Moskovits, M.; Stucky, G. D. *Nat. Mater.* **2004**, *3*, 816. (b) Platschek, B.; Keilbach, A.; Bein, T. *Adv. Mater.* **2011**, *23*, 2395.

(9) (a) Miao, Z.; Xu, D. S.; Ouyang, J. H.; Guo, G. L.; Zhao, X. S.; Tang, Y. Q. *Nano Lett.* **2002**, *2*, 717. (b) Limmer, S. J.; Cao, G. *Adv. Mater.* **2003**, *15*, 427. (c) Bian, S. W.; Ma, Z.; Song, W. G. *J. Phys. Chem. C* **2009**, *113*, 8668. (d) Liang, H. W.; Liu, S.; Yu, S. H. *Adv. Mater.* **2010**, *22*, 3925.

(10) For reviews, see: (a) Walter, M. G.; Warren, E. L.; McKone, J. R.; Boettcher, S. W.; Mi, Q.; Santori, E. A.; Lewis, N. S. *Chem. Rev.* **2010**, *110*, 6446. (b) Hagfeldt, A.; Boschloo, G.; Sun, L. C.; Kloo, L.; Pettersson, H. *Chem. Rev.* **2010**, *110*, 6595. (c) Peng, K. Q.; Lee, S. T. *Adv. Mater.* **2011**, *23*, 198.

(11) Zhang, Y. J.; Thomas, A.; Antonietti, M.; Wang, X. C. *J. Am. Chem. Soc.* **2009**, *131*, 50.

(12) (a) Würthner, F.; Thalacker, C.; Diele, S.; Tschierske, C. *Chem.—Eur. J.* **2001**, *7*, 2245. (b) Würthner, F.; Kaiser, T. E.; Saha-Möller, C. R. *Angew. Chem., Int. Ed.* **2011**, *50*, 3376.